

*Chapter VI*PROGRESS TOWARD TOUGHER PROTEIN HYDROGELS BY COMBINING CHEMICAL
AND PHYSICAL CROSS-LINKING**1. Abstract**

The combination of permanent covalent cross-links and reversible physical cross-links in polymeric hydrogels has been demonstrated to enhance the toughness and extensibility of these materials. These two types of interactions are present in chemical-physical hydrogels prepared by end-linking the triblock artificial protein EPE, which is capable of forming noncovalent, coiled-coil cross-links through the association of midblock domains within a covalent network. In this chapter, cross-linked EPE networks were tested in uniaxial tension to determine the stress and strain required to fracture the hydrogels. Two chemical networks were also prepared from the artificial proteins ERE and ER_CE, which differ in the number of cysteine residues available for covalent cross-linking. Hydrogels prepared from EPE could be extended further than both covalent hydrogels and also exhibited a greater work of extension, which is considered a measure of material toughness. These results demonstrate some progress toward engineering tougher, more extensible protein hydrogels by the incorporation of physical cross-linking by coiled-coil domains.

2. Introduction

Hydrogels are used widely in biomedical applications and consumer products due to their favorable elastic properties and their ability to absorb large amounts of water by swelling. However, the tendency for soft, highly swollen hydrogels to fracture easily imposes significant limitations on these applications. Absorption of solvent by swollen hydrogel networks decreases the polymer volume fraction, which in turn decreases the number of chains per unit area across a fracture surface. This results in the rupture of covalent bonds and the propagation of the fracture surface until the material fails. A number of strategies have been developed to overcome the weak, brittle nature of hydrogels and other polymeric materials. Many of these strategies have been reviewed recently [1, 2], and those that are most relevant to protein-based materials are discussed here.

A relatively simple approach to tough hydrogels is one that uses highly efficient covalent reactions to cross-link macromer precursors. This approach stands in contrast to what are termed conventional hydrogels that are polymerized from mixtures of small molecule monomers and cross-linkers. Conventional hydrogels are often characterized by heterogeneous network structures in which dense, tightly cross-linked regions are loosely connected by long polymer chains [1]. This can lead to very high amounts of stress per chain in the loosely cross-linked regions, which can contribute to fracture. An example of a more homogeneous hydrogel prepared by end-linking poly(ethylene) glycol (PEG) chains with a click reaction was reported by Hawker and coworkers [3]. In this work, bifunctional PEG alkyne chains and tetrafunctional PEG azide chains were linked together by the copper catalyzed azide-alkyne cycloaddition. The resulting hydrogel networks could be extended over 1500% and sustained true stresses of up to 2 MPa. In comparison, PEG hydrogels polymerized by conventional photochemical methods were significantly weaker and

less extensible. Similar homogeneous networks have been prepared by end-linking PEG macromers by Michael-type addition of thiols and vinyl sulfones [4] and by amide bond formation [5, 6]. This approach was also used in Chapter 2 to end-link ERE artificial protein chains with 4-arm PEG vinyl sulfone. Because proteins are monodisperse polymers, they are especially well-suited to forming homogeneous networks that may be tougher than conventional hydrogels.

Many recent strategies for developing tough hydrogels are based on the concept of dissipating energy by the incorporation of reversible or sacrificial cross-links. This strategy is perhaps best demonstrated by hydrogel networks containing polyacrylamide and alginate cross-linked within the same covalent network [7]. While polyacrylamide networks would normally be considered brittle conventional hydrogels, they were reinforced by ionic Ca^{2+} cross-links between the alginate chains. In this material design, the permanent covalent cross-links are proposed to maintain the shape and elasticity of the material while the ionic cross-links unzip reversibly to prevent the rupture of covalent bonds. Similar polymeric networks that have been described as tough include synthetic polyampholyte gels cross-linked by a pair of weak and strong ionic bonds [8], polyacrylamide-*co*-polyacrylic acid hydrogels containing Fe^{3+} ionic cross-links [9], triblock copolymers with poly(methylmethacrylate) endblocks and ionically cross-linked poly(methacrylic acid) midblocks [10], and poly(vinylpyridine) organogels with organometallic physical cross-links [11].

Coiled coils are candidates for the reversible or sacrificial cross-linking component in protein networks based on this toughening strategy. Compared to other protein structures including β -sheets, α -helical domains are considered mechanically weak with typical unfolding forces of tens of piconewtons as measured by single molecule force spectroscopy [12-14]. In protein hydrogels, the association of coiled coils as physical cross-linking domains is sufficiently weak

that these domains dissociate reversibly under thermal forces, resulting in viscoelastic behavior [15]. This suggests that they may be capable of dissipating energy during hydrogel deformation. Despite the potential of artificial proteins to participate in several different toughening mechanisms, to date there have been only a few research efforts in this area [16-19].

The initial motivation for preparing EPE chemical-physical hydrogels was to assess whether toughness and extensibility could be encoded within a polymeric material by programming the molecular association between artificial protein domains. In Chapter 3, it was shown that EPE could be used to prepare covalent hydrogel networks that also contained physical cross-links formed by the association of the helical domains on different protein chains. This behavior was clearly demonstrated in small angle oscillatory shear rheology experiments in which the transient physical cross-links resulted in a viscoelastic response to small strains. In this chapter, EPE hydrogels were stretched in uniaxial tension to determine the strain and stress at which these networks fracture. It was anticipated that the combination of the permanent covalent cross-linking and reversible physical cross-linking in EPE gels might result in toughening behavior that is analogous to the polyacrylamide-*co*-alginate network described by Sun *et al.* [7]. For comparison, two different chemical protein networks were also prepared with different cross-linking densities. The results described here demonstrate that the EPE network can be stretched further than either chemical network, but further experiments are required to conclude whether EPE chemical-physical networks can be classified as truly tough hydrogels.

3. Methods and Materials

3.1 Protein Synthesis

The EPE and ERE proteins were expressed and purified as described in the previous chapters and in Appendix B. The gene encoding the ER_CE protein was prepared by site-directed mutagenesis of the pQE-80L ERE plasmid using oligonucleotides reported in Appendix A. The resulting plasmid, pQE-80L ER_CE, was transformed into the BL21 strain of *Escherichia coli* and expressed and purified in the same way as ERE. The complete DNA and amino acid sequence of ER_CE is reported in Appendix A.

3.2 Preparation of Cross-linked Hydrogel Test Specimens

All hydrogels were prepared at 15 wt% total polymer and a 1:1 stoichiometry of vinyl sulfone and thiol functional groups. For tensile experiments, the proteins were cross-linked in a custom-designed, dumbbell-shaped mold with a narrow rectangular test region and wider tabs for improved gripping of the gel in the test fixture. The dimensions of the test region of the mold were 15 mm x 3 mm x 1 mm (L x W x H). Approximately 500 μ L of the cross-linking mixture was required to fill each mold. In a typical cross-linking experiment with EPE, 75 mg of protein was dissolved in 500 μ L of degassed cross-linking buffer (0.1 M sodium phosphate, 6 M guanidinium chloride, and 0.4 M triethanolamine, pH 7.4) by sonication for 1 min in an ultrasonic bath and centrifugation for 1 min at 10,000 *g*. The protein solution was combined with 115 μ L of PEG-4VS solution (150 mg mL⁻¹ in degassed 0.4 M triethanolamine, pH 7.4) and mixed quickly by vortexing. Approximately 500 μ L was pipetted into the dumbbell-shaped mold. The mixture was spread evenly and cured overnight at room temperature in a humidified chamber.

Cross-linked gels were removed from the mold and swollen in decreasing concentrations (6 M, 3 M, 2 M, 1 M) of guanidinium chloride in PBS (phosphate buffered saline, 1.5 mM KH₂PO₄,

4.3 mM Na₂HPO₄, 137 mM NaCl, 2.7 mM KCl, pH 7.4) over the course of approximately 30 hrs. The gels were then swollen in PBS containing 0.02% (w/v) sodium azide for 24-48 hr before uniaxial tensile testing or rheological testing.

3.3 Rheological Testing of As-Prepared and Swollen Hydrogels

Hydrogels were characterized by dynamic oscillatory shear rheology in the as-prepared and swollen states. The tests were performed on an ARES-RFS strain-controlled rheometer (TA Instruments). Hydrogel disks were loaded between 8 mm parallel plates as described in the previous chapters and in Appendix B. Frequency sweep experiments were performed from 100-0.1 rad s⁻¹ at 1% strain amplitude and 25 °C. Three replicates were performed for each gel.

3.4 Uniaxial Tensile Testing

Uniaxial tensile tests were performed on an Instron 5422 testing machine with a 5 N load cell. The instrument was controlled with the Bluehill3 software package (Instron). All tests were performed in an environmental chamber filled with buffer and maintained at 25 °C by a water jacket. The width of the swollen dumbbell hydrogels was measured with a digital caliper (Mitutoyo) and the thickness was measured with a digital micrometer (Mitutoyo). The gauge length was calculated by multiplying the measured width by 5 under the assumption that the gels swell isotropically. Hydrogels were prevented from slipping out of the grips by coarse sand paper. The tests were performed at a strain rate of 2 min⁻¹ (200% of gauge length per minute). To correct for the change in the buoyant force as the test fixture was raised out of the bath, the change in the volume of displaced buffer was calculated from the diameter of the cylindrical portion of the

fixture (3.13 mm). EPE, ERE, and ER_CE hydrogels were tested with the environmental chamber filled with PBS. Five replicates were performed for each protein gel. EPE and ERE gels were also tested under denaturing conditions. The gels were swollen in PBS containing 6 M guanidinium chloride for 24-48 hr and tested with the environmental chamber filled with the same buffer. Four EPE gels were tested and three ERE gels were tested (the fourth ERE gel broke during sample loading).

4. Results and Discussion

4.1 Protein Design and Synthesis

Three artificial proteins were designed to investigate the influence of coiled-coil physical cross-linking on the strength and extensibility of protein hydrogels. As described in Chapters 2 and 3, the artificial proteins ERE and EPE are triblock sequences containing elastin-like endblocks and terminal cysteine residues. Covalent hydrogels are formed from these proteins by end-linking with 4-arm poly(ethylene glycol) vinyl sulfone (PEG-4VS). EPE also contains a helical midblock domain P that forms homopentameric coiled coils with midblock domains on nearby chains. This association forms transient physical cross-links within the end-linked EPE network resulting in a chemical-physical hydrogel. In contrast, ERE contains a non-associative midblock domain R, and end-linking with PEG-4VS results in a chemical or covalent hydrogel. The viscoelastic properties and swelling behavior of ERE and EPE hydrogels are reported in Chapter 3. While ERE chemical networks store stress elastically, EPE hydrogels are viscoelastic due to the transient association of the physical cross-linking domains. When deformed, EPE hydrogels exhibit stress relaxation with a characteristic timescale of approximately 100 seconds. At shorter times ($t \ll 100$ s), energy or stress is stored within chain segments between both the chemical and physical cross-links. At

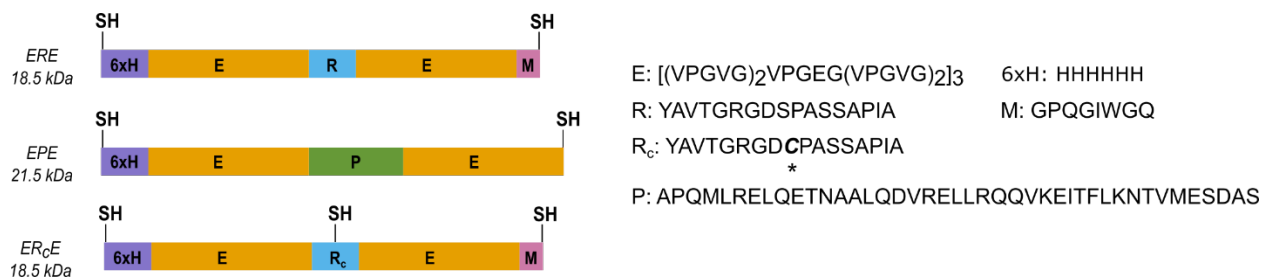


Figure VI-1. Sequences of artificial proteins EPE, ERE, and ER_cE. The multiblock structure is shown along with the sequences of each domain. The position of the serine to cysteine mutation in ER_cE is denoted by the * below the sequence.

longer times ($t \gg 100$ s), energy or stress is stored only within chain segments between the chemical cross-links. Because the physical cross-links occur within the middle of each end-linked EPE chain, the modulus at short times is approximately twice the modulus at long times. In other words, when a constant strain is applied, the amount of stress stored at short times is approximately twice the amount of stress stored at long times. As the stress relaxes, energy is dissipated as heat. In contrast, the stress stored in ERE hydrogels is nearly independent of time and little energy dissipation occurs.

EPE hydrogels are stiffer and more swollen than ERE hydrogels due to their increased cross-linking density. To understand how this might affect the tensile properties of protein networks, a second chemical hydrogel network was designed with the capacity to form an additional covalent cross-link at an internal cysteine residue located within the midblock domain R. This was accomplished by synthesizing a new artificial protein sequence by site-directed mutagenesis of the ERE gene to replace a serine residue within the R domain with a cysteine residue. The resulting protein, denoted ER_cE (Figure VI-1), differs from the ERE protein by a single atom; the oxygen of the Ser side chain is replaced by sulfur in the Cys side chain. However,

the introduction of an internal cross-linking site within the protein chain is expected to have a significant effect on the mechanical properties of materials prepared from this protein. It is anticipated that the increased covalent cross-linking density of ER_CE hydrogels will result in a modulus and polymer volume fraction that closely match the properties of EPE hydrogels. The capacity to precisely define covalent cross-linking sites in a polymer chain is a unique feature of genetically encoded artificial proteins.

4.2 Comparison of As-Prepared and Swollen EPE, ERE, and ER_CE Hydrogels

The three artificial proteins were cross-linked with PEG-4VS at an initial total polymer concentration of 15 wt% and a 1:1 vinyl sulfone to thiol stoichiometry. As in the previous chapters, cross-linking was performed under denaturing conditions in phosphate buffer containing 6 M guanidinium chloride. Because ER_CE contains three cysteine residues per chain, the fraction of PEG-4VS in the cross-linking reaction is higher than the fraction in the ERE and EPE reactions (28.6% for ER_CE, 21.3% for ERE, and 18.8% for EPE). The cross-linked gels were characterized in the as-prepared or unswollen state by dynamic oscillatory shear rheology. The storage moduli of the three gels are shown in Figure VI-2 a. EPE and ERE gels have nearly identical storage moduli (approximately 6 kPa) in the as-prepared state. This is expected because the two proteins have a similar molecular weight and identical sites for covalent cross-linking. The physical cross-linking domains in EPE gels are not expected to be associated in the as-prepared state because the cross-linking buffer contains protein denaturant. ER_CE gels are approximately twice as stiff as ERE and EPE gels in the as-prepared state. This is also expected because the additional cysteine cross-linking site in ER_CE occurs in the middle of the protein chain, cutting the average molecular weight between cross-links in half and doubling the modulus.

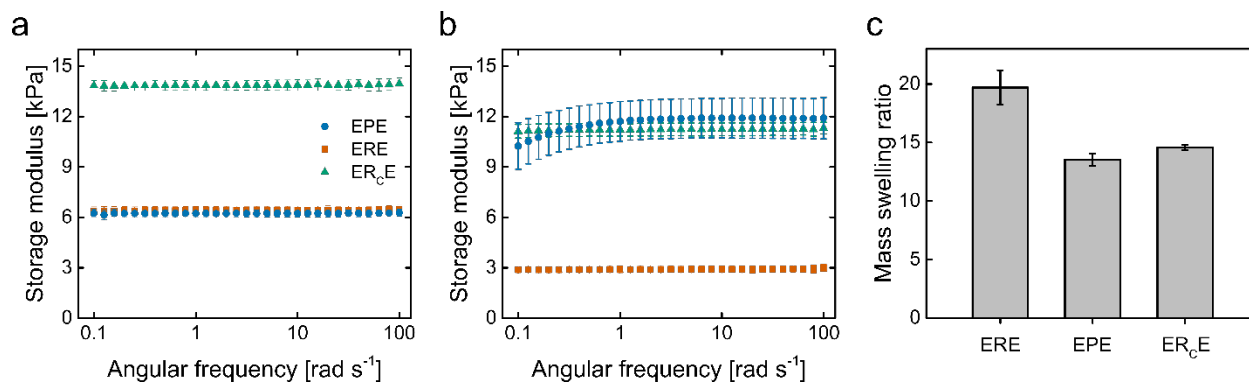


Figure VI-2. Rheology and swelling of EPE, ERE, and ER_cE hydrogels. Storage moduli ($n = 3$) in the as-prepared state (a) and after swelling to equilibrium in PBS (b) at 1% strain amplitude, 25 °C. (c) Mass swelling of the three protein hydrogels in PBS ($n = 6$).

The moduli of the hydrogels after swelling to equilibrium in phosphate buffered saline are quite different than in the as-prepared state (Figure VI-2 a and b). After removing the denaturant that was present during cross-linking, the midblock domains of EPE can associate with one another to form physical cross-links within the covalent network. As a result, the storage modulus of EPE in the swollen state is greater than the storage modulus in the as-prepared state despite a decrease in the polymer volume fraction. The viscoelastic behavior of the EPE hydrogels is also evident from the decrease in the storage modulus at lower frequencies. The frequency sweep experiments in Figure VI-2 were performed over an angular frequency range of 0.1-100 rad s⁻¹, so the long time or low frequency behavior described in Chapter 3 is not observed here. Unlike EPE gels, ERE and ER_cE hydrogels are softer in the swollen state than in the as-prepared state because the chain density decreases upon swelling and no additional cross-links are formed. The storage moduli of the ERE and ER_cE gels are approximately 3 kPa and 11 kPa, respectively. In contrast to the as-prepared state, the high frequency modulus of EPE gels in the swollen state is similar to the modulus of ER_cE gels rather than ERE gels. From these experiments, it is concluded that the rheological behavior of the three networks is consistent with the protein design and that these gels

can be used to compare the behavior of cross-linked protein networks with (1) no association between midblock domains, (2) physical or noncovalent association between midblock domains, and (3) chemically cross-linked midblock domains.

4.3 Uniaxial Tensile Testing of EPE, ERE, and ER_CE Hydrogels

Hydrogel specimens for tensile testing were prepared by cross-linking the three artificial proteins in dumbbell-shaped molds followed by swelling in decreasing concentrations of guanidinium chloride in PBS until the denaturant was removed. The swollen hydrogels (Figure VI-3) were clamped at the ends in the test fixture and extended in uniaxial tension at a strain rate of 2 min⁻¹ until failure. The tests were performed in a chamber filled with PBS and maintained at 25 °C. As the gels were stretched, the load was measured as a function of the hydrogel extension in order to calculate the engineering stress (force per initial cross-sectional area) and the engineering strain (the change in length divided by the initial length). Representative stress-strain curves for EPE, ERE, and ER_CE hydrogels are plotted in Figure VI-4. The hydrogels generally fractured away from the test fixture grips, with the exception of two ER_CE gels that broke very close to the bottom grip (Figure VI-5).

The stress to break (σ_b) and strain to break (ϵ_b) for five replicates of each gel are plotted in Figure VI-6 a and b. EPE hydrogels can be extended further than ERE or ER_CE gels before fracture. The stress required to fracture the EPE and ER_CE gels is similar, and is approximately 2-2.5 times greater than the stress required to fracture ERE gels. The work of extension (W_e), which is calculated by integrating the area under the stress-strain curve, is a measure of energy input as

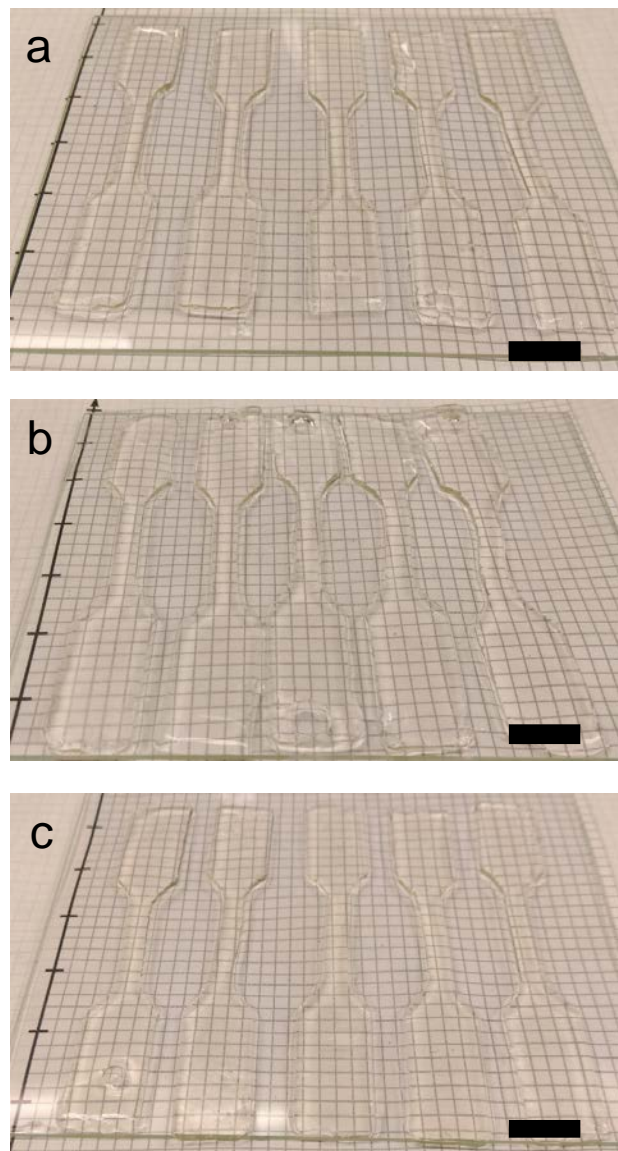


Figure VI-3. Swollen dumbbell-shaped hydrogels prior to tensile testing. (a) EPE (b) ERE (c) ER_cE. Scale bar 1 cm.

gel is stretched. As shown in Figure VI-6 c, EPE gels have a greater W_e than ERE or ER_cE gels. This difference may be related to the energy dissipated by the reversible physical cross-links. Finally, the Young's moduli of EPE and ER_cE are also similar (Figure VI-6 d), as expected based on the rheological experiments and swelling behavior indicating a similar cross-linking density. In contrast, ERE gels are softer and have a lower Young's modulus than EPE and ER_cE.

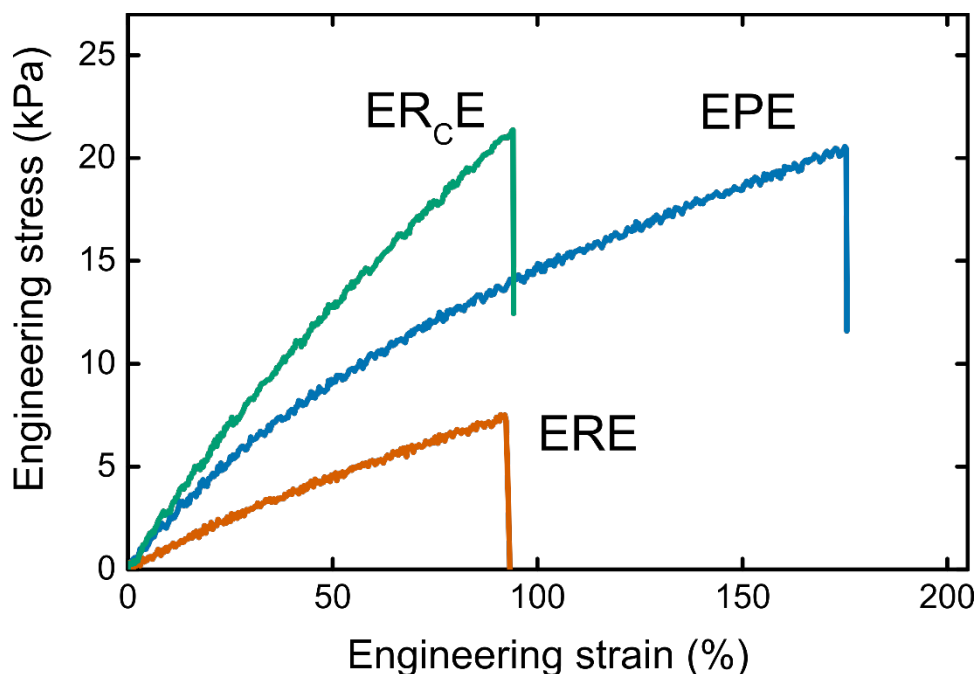


Figure VI-4. Representative stress-strain curves for EPE, ERE, and ER_cE hydrogels.

Concerning the toughness and extensibility of protein hydrogels, the most interesting feature to emerge from the tensile experiments is the increased strain to break for EPE chemical-physical networks relative to the ERE and ER_cE chemical networks. While EPE and ER_cE gels have similar fracture stresses, the stress-strain curves take different trajectories to reach this level of stress. For EPE gels, the slope of the stress-strain curve decreases at high strains, allowing the gel to be stretched further before rupturing. This effect is most likely due to either the viscoelasticity of the chemical-physical network or the forced mechanical unfolding of the physical cross-links at higher stress. Olsen *et al.* reported yielding behavior at a shear stress of 1.4 kPa in large amplitude oscillatory shear rheological experiments with physical protein hydrogels cross-linked by P coiled coils [20]. A similar phenomena may occur in EPE gels, with the unfolding of the physical cross-links between midblock domains preceding rupture of covalent bonds and material failure.

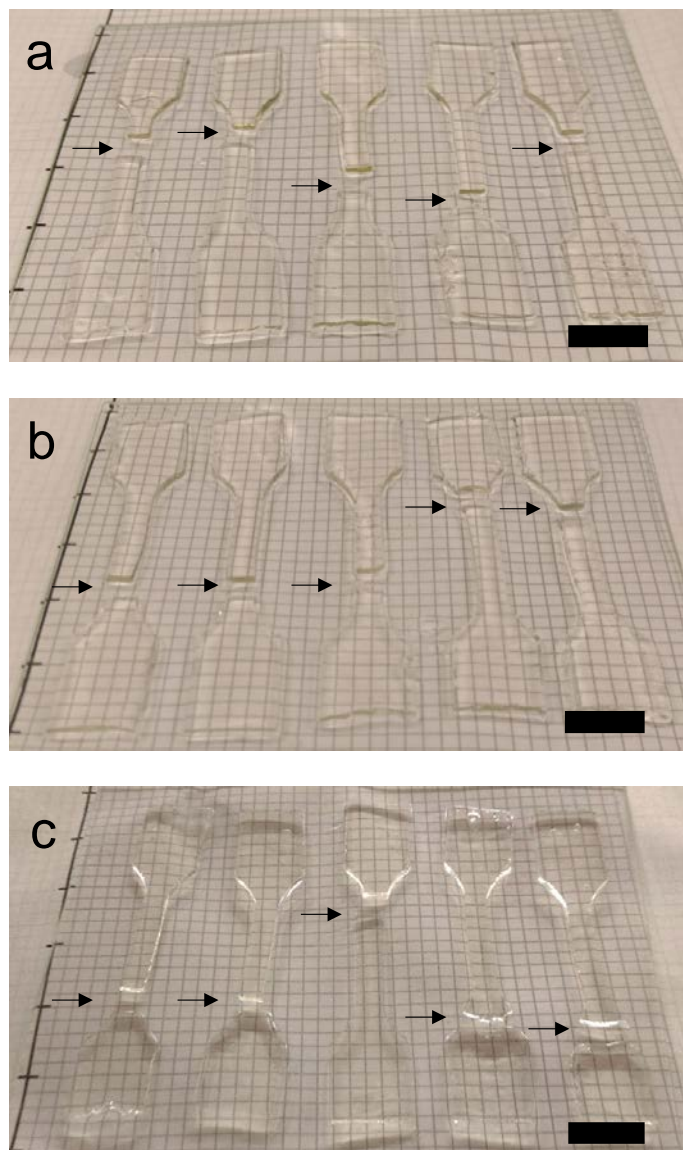


Figure VI-5. Swollen dumbbell-shaped hydrogels after tensile testing. (a) EPE (b) ERE (c) ER_cE. Arrows indicate the failure point in each gel. Scale bar 1 cm.

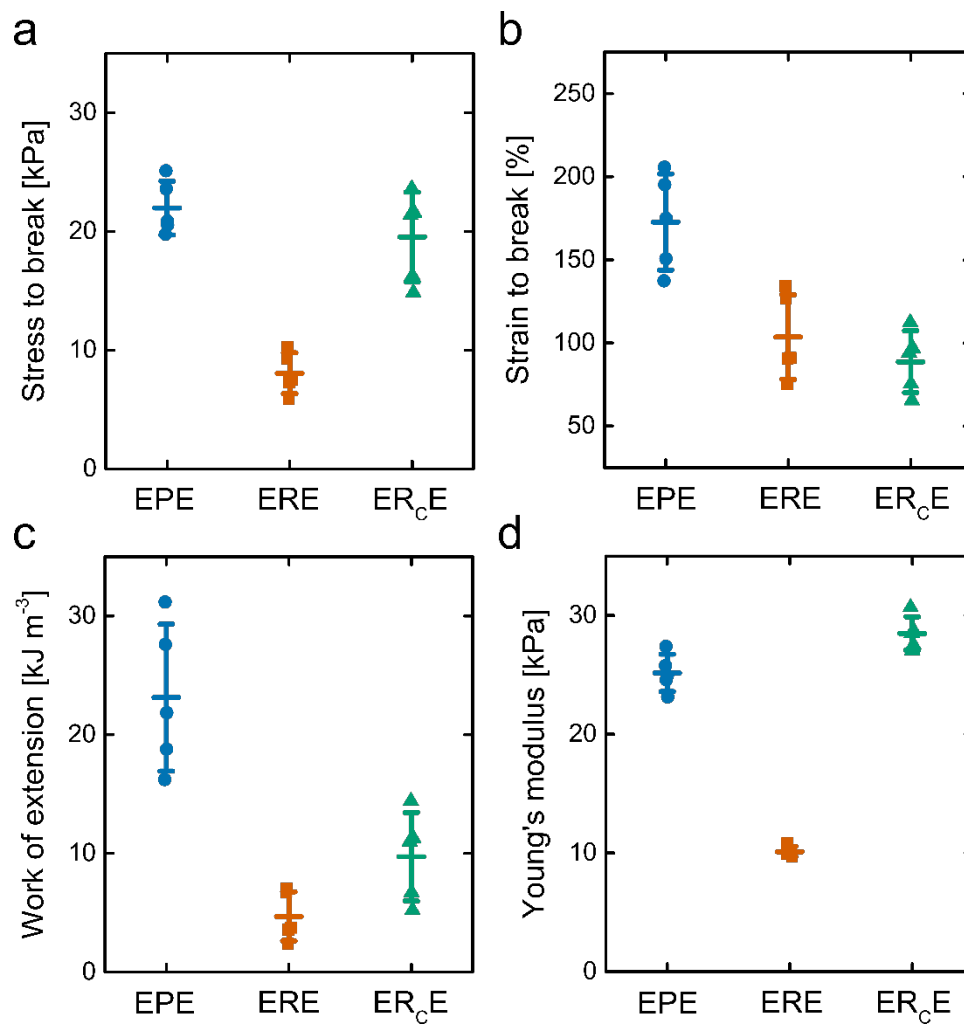


Figure VI-6. Tensile testing results for EPE, ERE, and ER_cE hydrogels. (a) Stress to break. (b) Strain to break. (c) Work of extension. (d) Young's modulus. The average values are shown by the dashes and error bars represent one standard deviation ($n = 5$ gels).

4.4 Tensile Testing of EPE and ERE Hydrogels under Denaturing Conditions

Rheological characterization and tensile testing were also conducted on EPE and ERE hydrogels swollen in denaturing buffer (6 M guanidinium chloride in PBS). Under these conditions, EPE and ERE gels have nearly identical storage moduli in the dynamic oscillatory frequency sweep experiments (2.7 and 2.9 kPa, respectively) (Figure VI-7). Like in the as-prepared state, EPE gels swollen in denaturant are not expected to exhibit physical cross-linking and should have a network structure that is similar to ERE gels. However, both EPE and ERE gels in denaturing buffer are softer than in the as-prepared state due to the decrease in the polymer volume fraction upon swelling.

The tensile tests for EPE and ERE gels swollen in denaturing buffer were performed with the environmental chamber filled with PBS containing 6 M guanidinium chloride. Stress-strain curves that are somewhat representative of the average behavior of EPE and ERE gels are shown in Figure VI-8. The average values of the stress to break, strain to break, work of extension, and the Young's modulus for EPE and ERE gels under denaturing conditions were not significantly different (Figure VI-9), suggesting that the tensile behavior of EPE gels in PBS may be attributable to the presence of physical cross-linking within the EPE network. However, it should be noted that there was considerable variability in the ERE gels, which together with the small sample sizes ($n = 4$ gels for EPE and 3 gels for ERE) makes it difficult to draw meaningful conclusions from this experiment. More replicates of each gel are required.

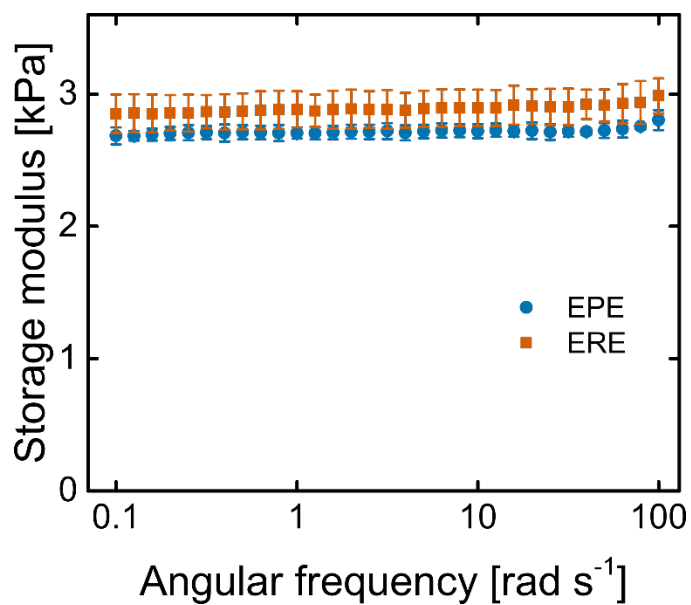


Figure VI-7. Rheology of EPE and ERE hydrogels under denaturing conditions (PBS with 6 M guanidinium chloride). 1% strain amplitude, 25 °C.

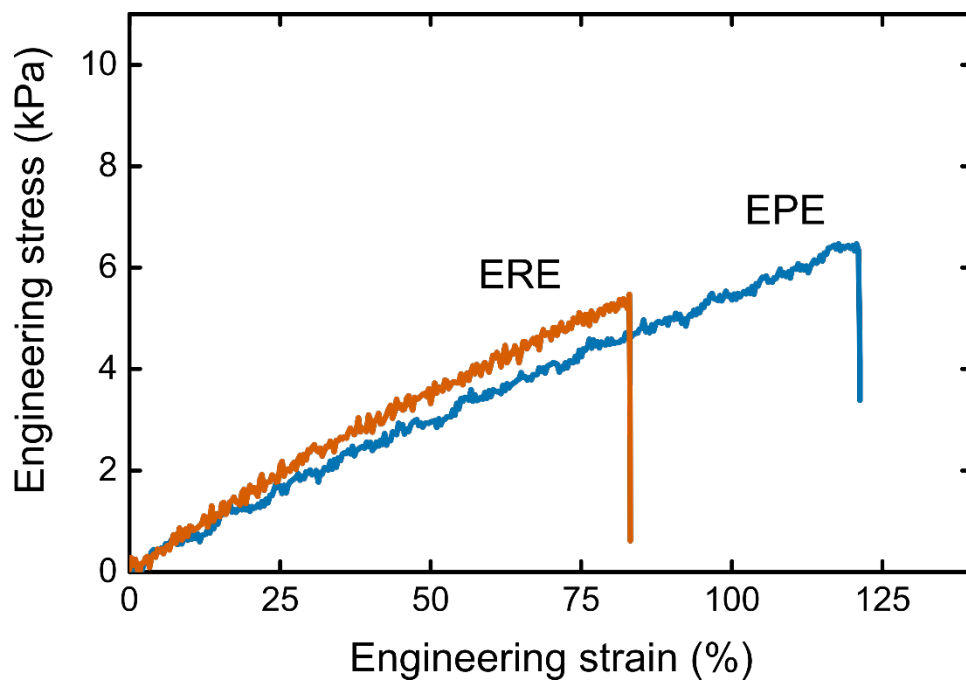


Figure VI-8. Representative stress-strain curves for EPE and ERE hydrogels under denaturing conditions (PBS with 6 M guanidinium chloride).

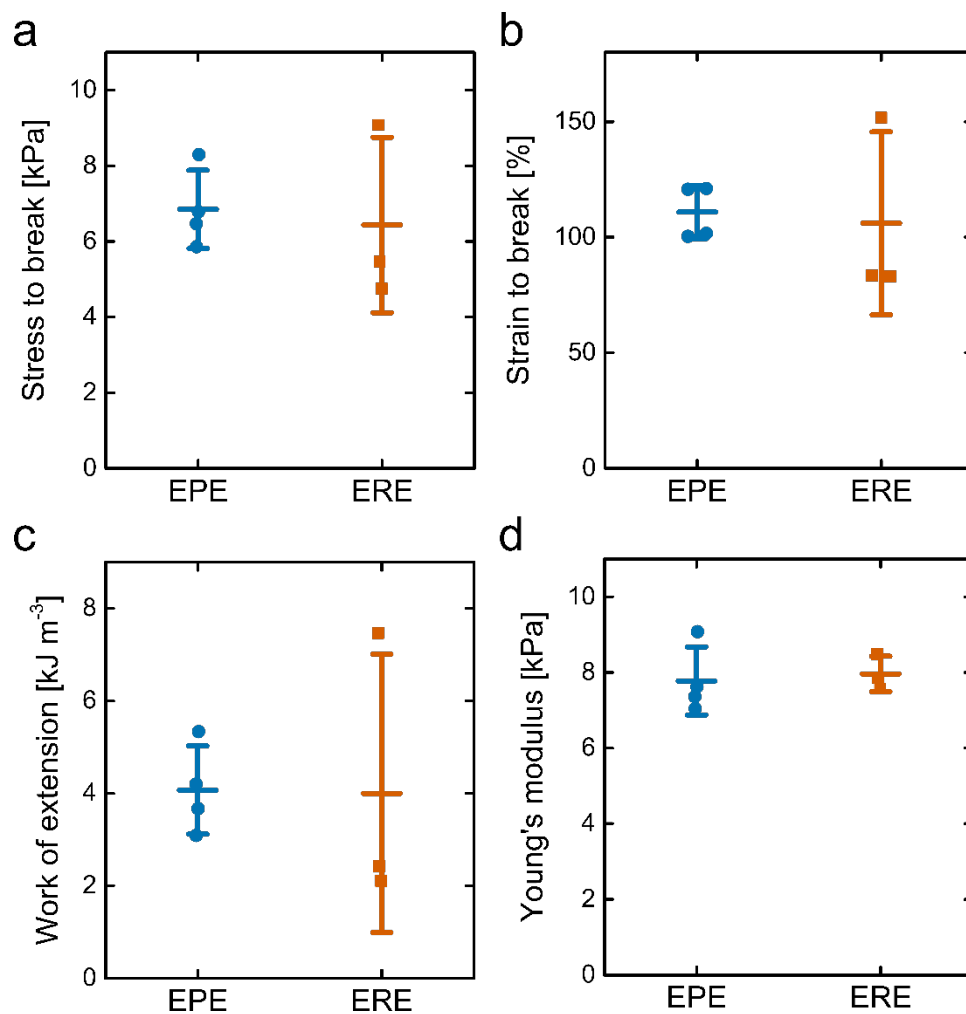


Figure VI-9. Tensile testing results for EPE and ERE hydrogels under denaturing conditions (PBS with 6 M guanidinium chloride). (a) Stress to break. (b) Strain to break. (c) Work of extension. (d) Young's modulus. The average values are shown by the dashes and error bars represent one standard deviation ($n = 4$ gels for EPE and 3 gels for ERE).

5. Future Experiments

Three further experiments are required to assess the toughness of the protein networks described in this chapter. First, loading-unloading cycles would provide a measure of the amount of energy that is recoverable after deformation and the amount of energy that is dissipated as heat. Based on rheological measurements, the viscoelastic EPE chemical-physical network is anticipated to dissipate more energy than the elastic ERE and ER_CE chemical networks. Preliminary measurements of EPE hydrogels indicate that up to 40% of the energy absorbed during loading is dissipated in a hysteresis loop. Cyclic strain experiments also provide a measurement of the fatigue of hydrogels after repeated loading and unloading. Many current hydrogel toughening strategies suffer from poor recovery after large strains because their sacrificial noncovalent cross-links are slow to reform after breaking. The fast recovery of physical protein hydrogels after large oscillatory strain and the short network relaxation timescales of hydrogels prepared from several EPE variants may prove useful for this purpose.

The effects of the network viscoelasticity on hydrogel toughness will be evaluated by performing tensile elongation to break experiments at different strain rates. Recent studies have suggested that deforming polymeric networks at strain rates that are much slower than the characteristic exchange time of transient physical cross-links results in enhancements to the fracture strain and fracture stress relative to faster strain rate experiments [11]. It may also be possible to address this issue by comparing the performance of hydrogels with different characteristic relaxation timescales prepared by the strategies described in Chapters 4 and 5.

Finally, tear tests including the trouser test and the pure shear test are regarded as better methods for evaluating the toughness of materials. These tests are used to determine the amount of energy required to generate a new surface by propagation of a defect or tear in the initial,

undeformed sample. Tough hydrogels typically have mechanisms for dissipating energy and preventing the propagation of defects so that the materials can be stretched further prior to failure. Whether these mechanisms exist in EPE hydrogels remains unclear. Preliminary trouser tear testing of an EPE hydrogel suggests that the fracture energy G_c is on the order of 10 J m^{-2} . While this value is greater than some conventional synthetic polymer hydrogels [1], it is still significantly lower than the values reported for double network hydrogels [21] and the polyacrylamide-*co*-alginate hydrogel [7].

6. Conclusions

Chemical-physical hydrogels prepared from the artificial protein EPE and chemical hydrogels prepared from the artificial proteins ERE and ER_cE were tested in uniaxial tension to determine their ultimate strength and elongation at break. Hydrogels prepared from EPE were the most extensible, with an average elongation of nearly 200%. They were also more extensible than ER_cE hydrogels despite having a similar stress to break. This may be due to either viscoelasticity of EPE hydrogels or to the mechanical unfolding or unzipping of the coiled-coil physical cross-links that has been described for several other tough hydrogels. EPE and ER_cE hydrogels also have similar moduli and swelling ratios, suggesting that the extensibility of protein networks can be tuned independently of other physical properties. Additional experiments have been proposed to determine whether EPE networks should be considered tough hydrogels and what the mechanism of toughening in these materials might be.

7. References

- [1] S. Naficy, H.R. Brown, J.M. Razal, G.M. Spinks, and P.G. Whitten *Aust. J. Chem.* **2011** *64*, 1007-1025.
- [2] X. Zhao *Soft Matter* **2014** *10*, 672-687.
- [3] M. Malkoch, R. Vestberg, N. Gupta, L. Mespouille, P. Dubois, A.F. Mason, J.L. Hedrick, Q. Liao, C.W. Frank, K. Kingsbury, and C.J. Hawker *Chem. Commun.* **2006** 2774-2776.
- [4] M.W. Tibbitt, A.M. Kloxin, L.A. Sawicki, K.S. Anseth *Macromolecules* **2013** *46*, 2785-2792.
- [5] Y. Akagi, J.P. Gong, U.-i. Chung, T. Sakai *Macromolecules* **2013** *46*, 1035-1040.
- [6] Y. Akagi, T. Katashima, Y. Katsumoto, K. Fujii, T. Matsunaga, U.-i. Chung, M. Shibayama, and T. Sakai *Macromolecules* **2011** *44*, 5817-5821.
- [7] J.-Y. Sun, X. Zhao, W.R.K. Illeperuma, O. Chaudhuri, K.H. Oh, D.J. Mooney, J.J. Vlassak, and Z. Suo *Nature* **2012** *489*, 133-136.
- [8] T.L. Sun, T. Kurokawa, S. Kuroda, A.B. Ihsan, T. Akasaki, K. Sato, M.A. Haque, T. Nakajima, and J.P. Gong *Nat. Mater.* **2013** *12*, 932-937.
- [9] P. Lin, S. Ma, X. Wang, F. Zhou *Adv. Mater.* **2015** *27*, 2054-2059.
- [10] K.J. Henderson, T.C. Zhou, K.J. Otim, K.R. Shull *Macromolecules* **2010** *43*, 6193-6201.
- [11] Z.S. Kean, J.L. Hawk, S. Lin, X. Zhao, R.P. Sijbesma, and S.L. Craig *Adv. Mater.* **2014** *26*, 6013-6018.
- [12] T. Bornschlöggl, J.C.M. Gebhardt, M. Rief *ChemPhysChem* **2009** *10*, 2800-2804.
- [13] T. Bornschlöggl, M. Rief *Phys. Rev. Lett.* **2006** *96*, 118102.
- [14] M.M. Stevens, S. Allen, J.K. Sakata, M.C. Davies, C.J. Roberts, S.J.B. Tendler, D.A. Tirrell, and P.M. Williams *Langmuir* **2004** *20*, 7747-7752.

- [15] W. Shen, J.A. Kornfield, D.A. Tirrell *Macromolecules* **2007** *40*, 689-692.
- [16] J. Fang, A. Mehlich, N. Koga, J. Huang, R. Koga, X. Gao, C. Hu, C. Jin, M. Rief, J. Kast, D. Baker, and H. Li *Nat. Commun.* **2013** *4*.
- [17] M.J. Glassman, R.K. Avery, A. Khademhosseini, B.D. Olsen *Biomacromolecules* **2016** *17*, 415-426.
- [18] S. Lv, D.M. Dudek, Y. Cao, M.M. Balamurali, J. Gosline, and H. Li *Nature* **2010** *465*, 69-73.
- [19] S. Tang, M.J. Glassman, S. Li, S. Socrate, and B.D. Olsen *Macromolecules* **2014** *47*, 791-799.
- [20] B.D. Olsen, J.A. Kornfield, D.A. Tirrell *Macromolecules* **2010** *43*, 9094-9099.
- [21] J.P. Gong *Soft Matter* **2010** *6*, 2583-2590.